Cell

Anchorage of Microtubule Minus Ends to Adherens Junctions Regulates Epithelial Cell-Cell Contacts

Wenxiang Meng,[1] Yoshimi Mushika,[1,2] Tetsuo Ichii,[1,3] and Masatoshi Takeichi[1,*]
[1]RIKEN Center for Developmental Biology, Chuo-ku, Kobe 650-0047, Japan
[2]Graduate School of Biostudies, Kyoto University, Yoshida-Honmachi, Sakyo-ku, Kyoto 606-8501, Japan
[3]Present address: ERATO, JST, Osaka University, Suita, Osaka 565-0871, Japan
*Correspondence: takeichi@cdb.riken.jp
DOI 10.1016/j.cell.2008.09.040

SUMMARY

Epithelial cells contain noncentrosomal microtubules (MTs), whose minus ends are oriented apically. In contrast with the well-known interactions of the minus ends with the centrosome, little is known about the termination site of the noncentrosomal minus ends. Here we show that a population of MT minus ends is anchored at the zonula adherens (ZA), the apical-most part of the cadherin-based adherens junction, via a protein that we have termed Nezha. We initially identified PLEKHA7 as a ZA component and subsequently detected Nezha as a partner for PLEKHA7. Nezha bound MTs at their minus ends and tethered them to the ZA. Furthermore, we found that a minus end-directed motor, KIFC3, was concentrated at the ZA in a PLEKHA7/Nezha/MT-dependent manner; and depletion of any of these proteins resulted in disorganization of the ZA. We propose that the PLEKHA7/Nezha/MT complex regulates the ZA integrity by recruiting KIFC3 to this junctional site.

INTRODUCTION

Microtubules (MTs) are a major component of the cytoskeleton, and they play important roles in various cellular processes. In many cell types, MTs are organized in a radial array with their minus ends anchored at the centrosome and their plus ends extending toward the cell periphery where they play a number of biological roles (Akhmanova and Hoogenraad, 2005). On the other hand, many types of terminally differentiated cells contain a substantial number of noncentrosomal MTs, in addition to the centrosomal ones (Bartolini and Gundersen, 2006). In polarized epithelial cells, the former are arranged along the apicobasal axis of the cell with their minus ends oriented apically and their plus ends basally (Bacallao et al., 1989). Where these minus ends terminate and what cellular processes are regulated by the noncentrosomal minus ends are, however, largely unknown (Dammermann et al., 2003).

MTs are known to interact with the cell-cell adhesion machinery. Cell junctions of epithelial cells comprise the tight junction, adherens junction (AJ), and desmosome, which together form the junctional complex at the apical end of the lateral cell-cell contacts of these cells (Vogelmann and Nelson, 2005). The AJs are organized by cadherins and associated cytoplasmic proteins, including β-catenin and p120-catenin; and these AJs form the "zonula adherens" (ZA) or "adhesion belt," which enclose the polarized epithelial cells at their near-apical end, together with the underlying actin fibers. Recent studies showed that MT plus ends terminated at the AJs of mammary tumor cells and that MT depolymerization caused disorganized accumulation of E-cadherin in these cells (Stehbens et al., 2006), as observed earlier with other cells (Waterman-Storer et al., 2000), suggesting that MTs are required for AJ assembly. In addition, N-cadherin was found to be transported to the plasma membrane, dependent on MT networks as well as MT-based motors (Mary et al., 2002; Teng et al., 2005). The M-cadherin-catenin complex was also shown to interact with MTs (Kaufmann et al., 1999). Other studies showed that β-catenin bound dynein, which may play a role in tethering MTs at the AJs (Ligon et al., 2001) and that this tethering of MT plus ends at the AJs promoted the delivery of connexin hemichannels to the cell-cell border (Shaw et al., 2007). Although most of these studies suggest that MT plus ends interact with cell junctions, another study reported that N-cadherin-mediated adhesion stabilized the minus ends (Chausovsky et al., 2000).

To further explore the functional and structural relationships between the AJ and MTs, we paid particular attention to p120-catenin (p120) because we and others earlier found that p120 had the ability to associate with MTs (Chen et al., 2003; Franz and Ridley, 2004; Ichii and Takeichi, 2007; Yanagisawa et al., 2004). For example, when p120-GFP was overexpressed in cells, this construct became associated with MTs in an N-terminal region-dependent manner (Ichii and Takeichi, 2007). These observations raise the possibility that, in the natural setting, p120 coupled with cadherin might also interact with MTs, presumably with this interaction being mediated by other proteins. To test this possibility, in this present study we searched for proteins interacting with the p120 N-terminal region and identified a novel molecule, PLEKHA7 (pleckstrin homology domain-containing, family A member 7) (Gerhard et al., 2004;

Strausberg et al., 2002). We subsequently identified another novel protein, which we designated as Nezha (a deity in Chinese mythology), as a binding partner for PLEKHA7. These two proteins were localized along the ZA but not at the other parts of the AJ. Unexpectedly, we found Nezha to be associated with the minus ends of MTs, supporting the idea that the cadherin-p120 complex or AJ is linked with MTs, but via their minus ends rather than via their plus ones.

The above form of MT-ZA association prompted us to hypothesize that minus end-directed motors may utilize these MTs as a track for reaching the ZA. In fact, we found that one of the kinesin-14 family members, KIFC3, was concentrated in the ZA and that its junctional localization was abolished by RNAi-mediated depletion of PLEKHA7 or Nezha. Depletion of PLEKHA7, Nezha, or KIFC3 also resulted in disorganization of the ZA. Thus, we found a novel MT minus-end-anchoring mechanism, as well as one of its functions, which was important to maintain the integrity of the ZA.

RESULTS

Identification of PLEKHA7 as a p120-Catenin Partner

To search for proteins interacting with the N-terminal region of p120-catenin (p120), we generated a GST fusion protein for this domain (N-GST) or an N-terminus-deleted p120 (ΔN-GST; Figure 1A) and incubated them with lysates of human colon carcinoma Caco2 cells. Mass spectrometric analysis of the materials pulled down with these fusion proteins showed that an isoform of PLEKHA7 specifically cosedimented with the p120 N-terminal domain. PLEKHA7 is a protein that has WW, PH (pleckstrin homology), and CC (coiled-coil) domains (Figure 1B), but its biological function has not been characterized yet. To confirm the binding of PLEKHA7 with the p120 N-terminal domain, we constructed a Flag-tagged PLEKHA7 (PLEKHA7-Flag) and transfected Caco2 cells with this construct. The lysates of these transfectants were then incubated with N-GST, ΔN-GST, or GST. The results of this pull-down assay showed that PLEKHA7-Flag was precipitated only with the N-GST (Figure 1C). Next, we used a lysate of the above PLEKHA7-Flag or control transfectants to examine whether this PLEKHA7-Flag could be coimmunoprecipitated with endogenous p120, and we found that anti-Flag antibodies could cosediment p120 only from the PLEKHA7-Flag transfectants (Figure 1D). The immunoprecipitates from the PLEKHA7-Flag transfectants also contained E-cadherin (Figure 1D), as well as α- and β-catenin (data not shown), suggesting that PLEKHA7 was associated with the E-cadherin-catenin complex via p120. Further analysis determined that a portion from aa 538 to 696 of PLEKHA7 was required for its binding to p120 (Figure S1 available online).

Next, we generated antibodies against human PLEKHA7. These antibodies recognized two bands with molecular masses of 135 kDa and 145 kDa in western blots (Figure S2A), of which the 135 kDa band was the dominant one. Immunofluorescence staining of Caco2 cells showed that PLEKHA7 was localized along cell-cell junctions (Figure 1E). In Caco2 cell-cell junctions, an earlier study showed that there are two populations of E-cadherin: one is linearly localized along the apical-most portion of the junction, corresponding to the ZA, and the other is distributed as a meshwork or puncta at the lower portions of the junction (Otani et al., 2006). Double-immunostaining for PLEKHA7 and E-cadherin revealed that PLEKHA7 was localized only along the ZA (Figure 1E). A similar localization of PLEKHA7 was observed in other epithelial cell lines, as well as in embryonic epithelial and neural tissues (data not shown). PLEKHA7 was also detected in the centrosomes (Figure S2B).

To confirm whether the above PLEKHA7 distribution was mediated by p120, we examined the effect of p120 depletion. At the junctions of p120 siRNA-treated Caco2 cells, PLEKHA7 was reduced in simple proportion to the reduction of p120 level (Figure S3A). E-cadherin localization was also affected in these cells, as expected from earlier observations (Reynolds, 2007). However, E-cadherin level declined in a fashion less sensitive to the p120 reduction than that of PLEKHA7 (Figure S3A), suggesting that only the latter was proportional to the p120 level. To further corroborate the involvement of p120, we used cadherin-deficient Neuro-2a cells (Ichii and Takeichi, 2007). These cells were transfected with a normal cadherin, or its mutant cN/JM(-), in which the p120-binding region had been deleted (Aono et al., 1999). In the normal cadherin transfectants, PLEKHA7 was recruited to the cell-cell contact sites, whereas this did not occur in the mutant transfectants (Figure S3B). These observations support the idea of the p120-dependent recruitment of PLEKHA7 to the junctions.

PLEKHA7 Regulates Zonula Adherens Integrity

To explore the functions of PLEKHA7, we first exogenously expressed PLEKHA7-GFP in Caco2 cells and found that this construct was also selectively localized along the ZA. Intriguingly, the overexpressed PLEKHA7 molecules upregulated the level of E-cadherin accumulating at the ZA while concomitantly downregulating its level at the lower portions of the junction (Figure 1F). The junctional localization of p120 and other catenins responded to the PLEKHA7 overexpression in a similar fashion (data not shown), suggesting that excess PLEKHA7 redistributed the E-cadherin-catenin complex to the ZA, removing it from the lower portions of the cell junction.

Next, we knocked down the expression of PLEKHA7 in Caco2 cells by using siRNAs specific for this molecule. The overall level of PLEKHA7 in the culture was significantly reduced by the siRNA treatment (Figure S2C). After depletion of PLEKHA7, the intensity of E-cadherin signals distributed along the ZA was strongly reduced; whereas the lower lateral components of E-cadherin were not much affected (Figure 1G). p120 and α- and β-catenin were also eliminated from the ZA (data not shown). The circumferential actin belts remained intact along the ZA after PLEKHA7 depletion, although disassembled actin fibers were more frequently observed (Figure S2D); and the accumulation of ZO-1 and desmoplakin, markers for tight junction and desmosome, respectively, was not particularly altered by PLEKHA7 depletion (Figure S2E). These observations suggest that PLEKHA7 was specifically important for the cadherin-catenin accumulation at the ZA.

PLEKHA7 Binds Nezha, a Novel Protein Localizing at the Zonula Adherens

In order to investigate the mechanisms for the PLEKHA7-dependent regulation of cadherin assembly, we conducted

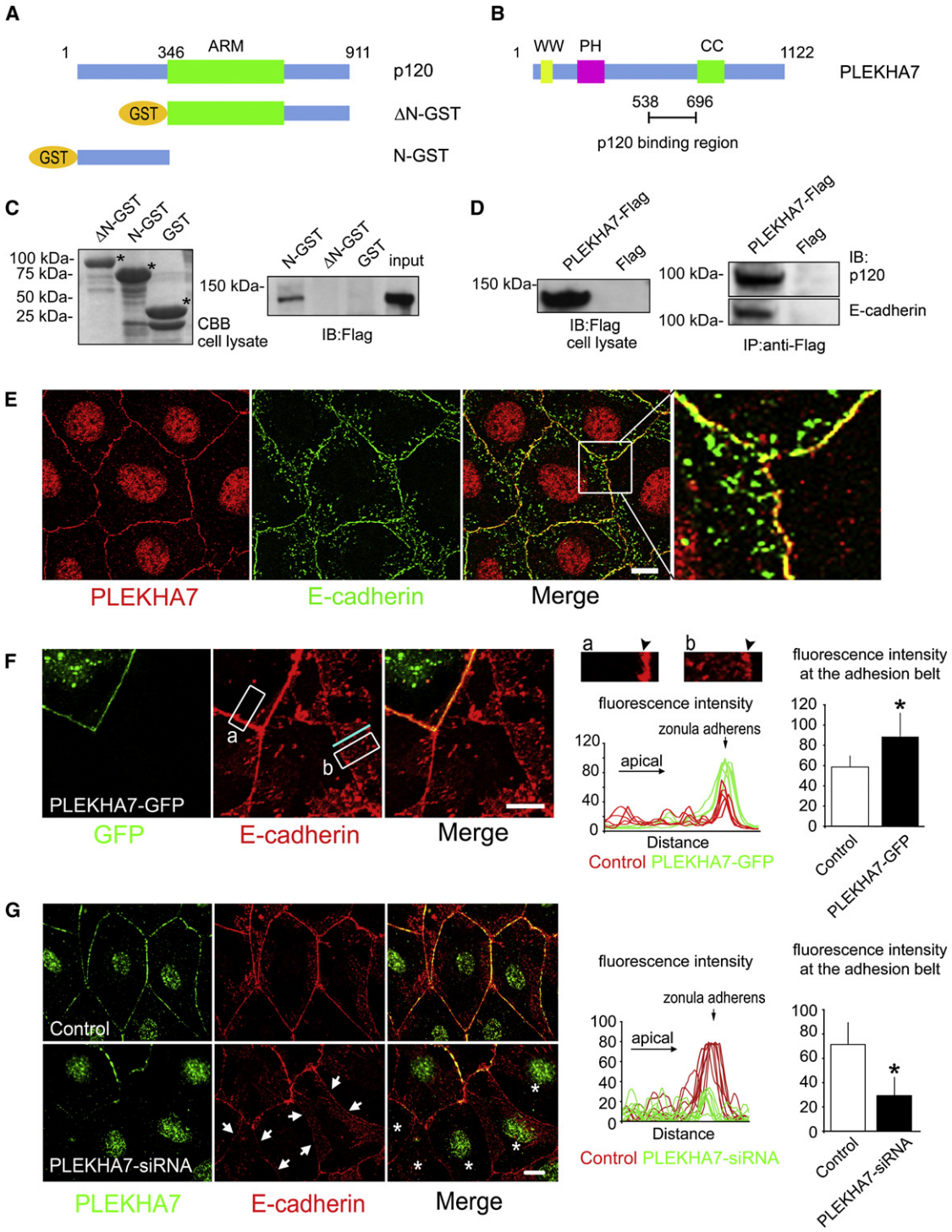

Figure 1. PLEKHA7 Associates with p120 and Localizes at the Zonula Adherens

(A) Structural views of mouse p120 and its fusion constructs with GST. ARM, armadillo domain.

(B) Structural view of human PLEKHA7.

(C) In vitro interactions of the p120 N-terminal domain with PLEKHA7. GST-fusion proteins (left, asterisks) were incubated with a lysate of Caco2 cells transiently transfected with PLEKHA7-Flag and then pulled down with Glutathione-Sepharose 4B beads. Coprecipitated materials were detected with anti-Flag antibodies (right).

(D) PLEKHA7 associates with p120 and E-cadherin. Caco2 cells were transiently transfected with PLEKHA7-Flag or control vector, and then their lysates (left) were subjected to immunoprecipitation with anti-Flag antibodies. In the immunoprecipitates, p120 and E-cadherin were detected by immunoblotting (right).

pulldown assays using PLEKHA7-GST fusion proteins to screen for proteins that interact with PLEKHA7. One construct comprising GST and a PLEKHA7 fragment (from aa 680 to 821) corresponding to its CC domain (Figure S4A) interacted with an as yet uncharacterized 150 kDa protein (KIAA1543), and we termed this protein Nezha. Nezha comprises one calponin homology (CH) and two coiled-coil (CC1 and 2) domains, as well as one DUF1781 (DUF) domain of unknown function (Figure 2A). We generated antibodies against Nezha. Western blot analysis of Caco2 cell lysates with these antibodies detected two bands, a major one with a molecular mass of 150 kDa and a minor one of 160 kDa (Figure 2A); and these bands became undetectable after RNAi-mediated depletion of Nezha, assuring the specificity of the antibodies (see Figure 2E). Next, we examined, by using a lysate of Caco2 cells doubly transfected with PLEKHA7-Flag and EGFP-tagged Nezha (Nezha-GFP) or control EGFP, whether Nezha could be coimmunoprecipitated with PLEKHA7 and found that anti-GFP antibodies precipitated PLEKHA7-Flag only from the Nezha-GFP transfectants (Figure 2B). We further found that anti-Nezha antibodies not only precipitated endogenous Nezha itself but also coprecipitated endogenous PLEKHA7 (Figure 2C). Deletion analysis of Nezha showed that the C-terminal region from aa 943 to 1225 contained the site required for its association with PLEKHA7 (Figure S4B).

In immunofluorescence staining of Caco2 cells, Nezha was detected as punctate signals scattered in the cytoplasm, but this protein was also localized along the ZA together with PLEKHA7 (Figure 2D). This junctional localization of Nezha became detectable only at mature cell-cell contacts, e.g., at 3 days under the present culture conditions (see Experimental Procedures), whereas PLEKHA7 appeared by 1 day. To examine whether the distribution of Nezha could be regulated by PLEKHA7, we depleted PLEKHA7 by treating Caco2 cells with specific siRNAs and found that the Nezha signals disappeared from the cell junctions, but not from the cytoplasm (Figure 2D), suggesting that the junctional localization of Nezha, but not the cytoplasmic one, was dependent on PLEKHA7. Reciprocally, when Nezha had been depleted by siRNAs specific for this protein, the PLEKHA7 distribution pattern became irregular; and the ZA-associated E-cadherin became reduced and discontinuous (Figures 2E and 2F). These observations suggest that Nezha, once associated with PLEKHA7, serves to maintain the integrity of the ZA. As found for PLEKHA7, Nezha depletion did not affect ZO-1 accumulation (see Figure S11).

Nezha Binds with MTs at the Minus Ends

To explore the biological functions of Nezha, we constructed a series of Nezha deletion mutants tagged with EGFP and transfected Caco2 cells with their cDNAs (Figure S5A). Immunostaining for EGFP and α-tubulin suggested that overexpressed Nezha was associated with MTs, inducing their bundling, and that this MT-bundling ability of Nezha required the C-terminal region (Figure S5A), which also contained the PLEKHA7-binding site, as mentioned already (Figure S4). For biochemical confirmation of the Nezha-MT interaction, we prepared an extract of Caco2 cells and added carrier tubulins and then Taxol (pacilitaxel) to the solution, according to a method previously described (Vallee, 1982). The MT pellets collected from this extract contained Nezha (Figure S5B). When a recombinant Nezha-Flag was mixed with purified tubulins, these proteins also coprecipitated (Figure S5C), strongly suggesting that Nezha could directly bind MTs.

These observations prompted us to analyze the cytological relationship between endogenous Nezha and MTs. We double-immunostained for these two molecules in Caco2 cells and found that the Nezha signals were mostly localized at one end of noncentrosomal MTs (Figure 3A). To characterize this localization, we triple-immunostained for MTs, Nezha, and EB1, a protein known to bind exclusively to the MT plus end (Mimori-Kiyosue et al., 2000; Su et al., 1995). Strikingly, Nezha and EB1 were distributed differently (Figure 3B), and high-magnification images showed that these two proteins were localized at the opposite ends of noncentrosomal MTs (Figure 3C). These results suggest that Nezha bound to the minus end of noncentrosomal MTs. On the other hand, Nezha was not detected at the centrosomes marked by γ-tubulin staining (Figures S6A and S6B), except that overexpressed Nezha recruited γ-tubulin onto Nezha-induced MT bundles (Figure S6C). It is known that ninein, a centrosomal minus-end capping protein, is released from the centrosomes and redistributed to the apical cortex of cells (Mogensen et al., 2000) or desmosomes (Lechler and Fuchs, 2007) and that these ninein molecules anchor MTs at these respective sites, like Nezha. However, double-immunostaining for ninein and Nezha showed that their distributions did not overlap (Figure S7). Desmoplakin depletion also did not affect the junctional localization of Nezha (data not shown).

To further characterize the minus-end-specific binding nature of Nezha, we performed an in vitro MT-capping experiment (Wiese and Zheng, 2000). For this assay, we chose a C-terminal-half fragment of Nezha (Nezha-CC1F), whose MT-bundling ability was cytochemically indistinguishable from that of the full-length

(E) Double-immunostaining for endogenous PLEKHA7 and E-cadherin in Caco2 cells. The boxed area is enlarged in the rightmost panel. Nuclear signals seen in this and other panels are thought to be nonspecific ones unique to our rabbit anti-PLEKHA7 pAbs, as these signals were unchanged after PLEKHA7 depletion.
(F) PLEKHA7 overexpression enhances E-cadherin distribution at the ZA. Exogenous PLEKHA7-GFP, introduced into Caco2 cells, and E-cadherin were double-immunostained in a mixed culture of GFP-positive and -negative cells. The two boxed areas are enlarged at the right, where exogenous PLEKHA7 is expressed in "a" but not in "b." Arrowheads indicate the ZA. Relative fluorescence intensity of E-cadherin signals distributed from the basal-most to apical-most portions was measured, choosing tilted junctions, and the fluorescence was scanned along the apicobasal lines (n = 5) drawn at random positions, one of which is shown in cyan as an example. The fluorescence value at the ZA was compared in the presence and absence (control) of exogenous PLEKHA7. *$p < 0.01$, n = 3 independent experiments (50 cells/n). Error bars represent the standard deviation (SD). The E-cadherin level was quantified in this way also in other figures.
(G) PLEKHA7 depletion downregulates E-cadherin accumulation at the ZA. Caco2 cells were transiently transfected with control or PLEKHA7 siRNA, and PLEKHA7 and E-cadherin were then double-immunostained. In the ZA of PLEKHA7-depleted cells (asterisks), E-cadherin signals are reduced (arrows). *$p < 0.01$, n = 3 independent experiments (50 cells/n). Error bars represent the SD.
Scale bars: 10 μm.

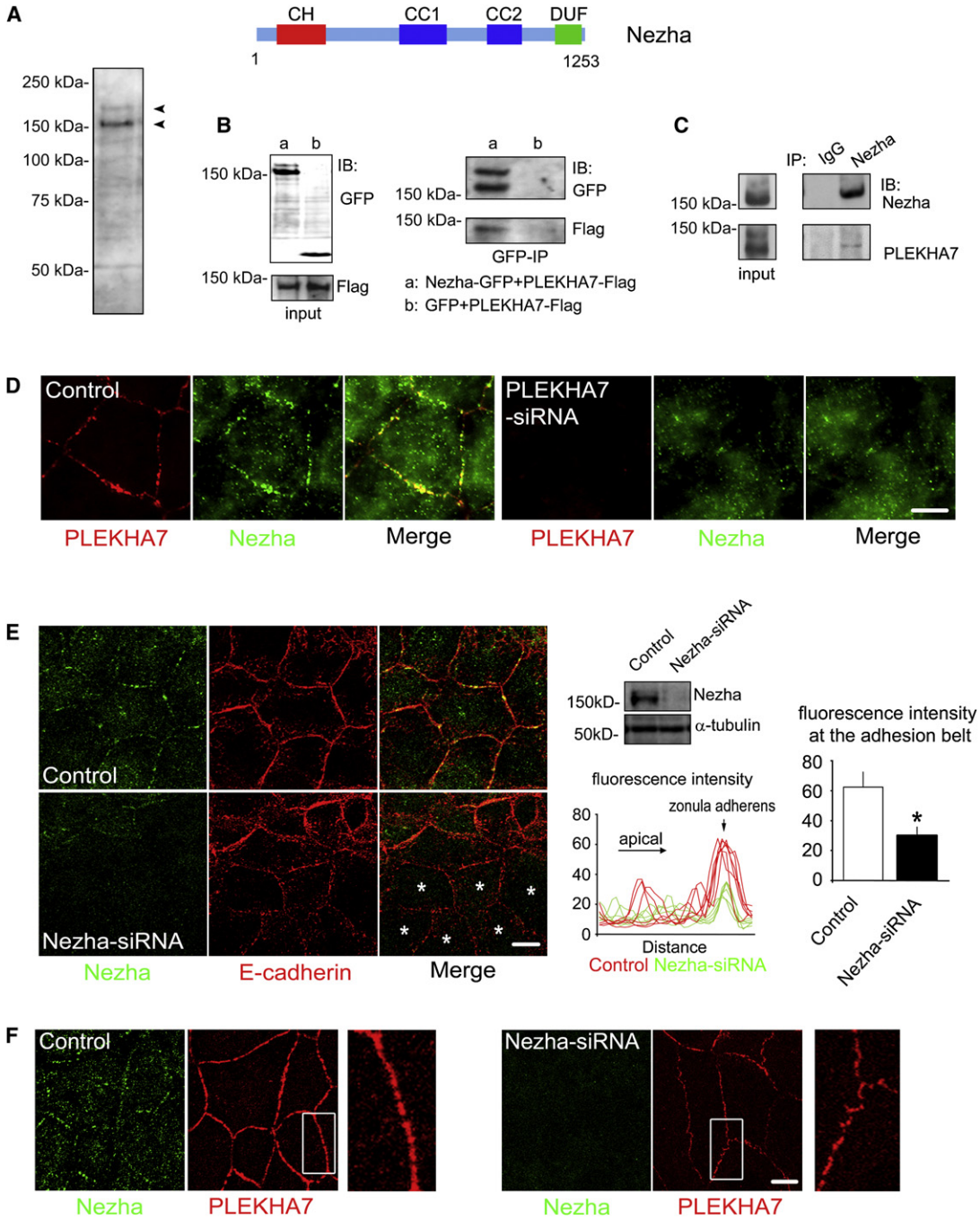

Figure 2. Nezha Interacts with PLEKHA7 and Regulates E-Cadherin Assembly

(A) Immunoblot detection of Nezha in Caco2 cells, and a structural view of human Nezha.

(B) Interaction of PLEKHA7 and Nezha. Caco2 cells were transiently transfected with PLEKHA7-Flag and Nezha-GFP or control GFP vector (left), and their lysates were subjected to immunoprecipitation with anti-GFP antibodies. The immunoprecipitates were then analyzed with anti-GFP and anti-Flag antibodies (right).

(C) Coimmunoprecipitation of endogenous Nezha and PLEKHA7 with anti-Nezha antibodies obtained from a Caco2 cell lysate.

(D) Endogenous Nezha and PLEKHA7 are colocalized at the ZA, and the junctional distribution of Nezha is PLEKHA7 dependent. Caco2 cells were transfected with control or PLEKHA7 siRNA and then double-immunostained for PLEKHA7 and Nezha. Only the junctional Nezha signals disappear after PLEKHA7 depletion.

(E and F) Nezha depletion perturbs E-cadherin (E) and PLEKHA7 (F) localization. Caco2 cells were transfected with control or Nezha siRNA and subsequently double-immunostained for Nezha and E-cadherin or PLEKHA7. Asterisks mark Nezha-depleted cells. The siRNA-dependent Nezha depletion was confirmed by immunoblotting. The E-cadherin level at the ZA was quantified. *$p < 0.01$, $n = 3$ independent experiments (50 cells/n). Error bars represent the SD. The boxed areas are enlarged at the right.

Scale bars: 5 μm.

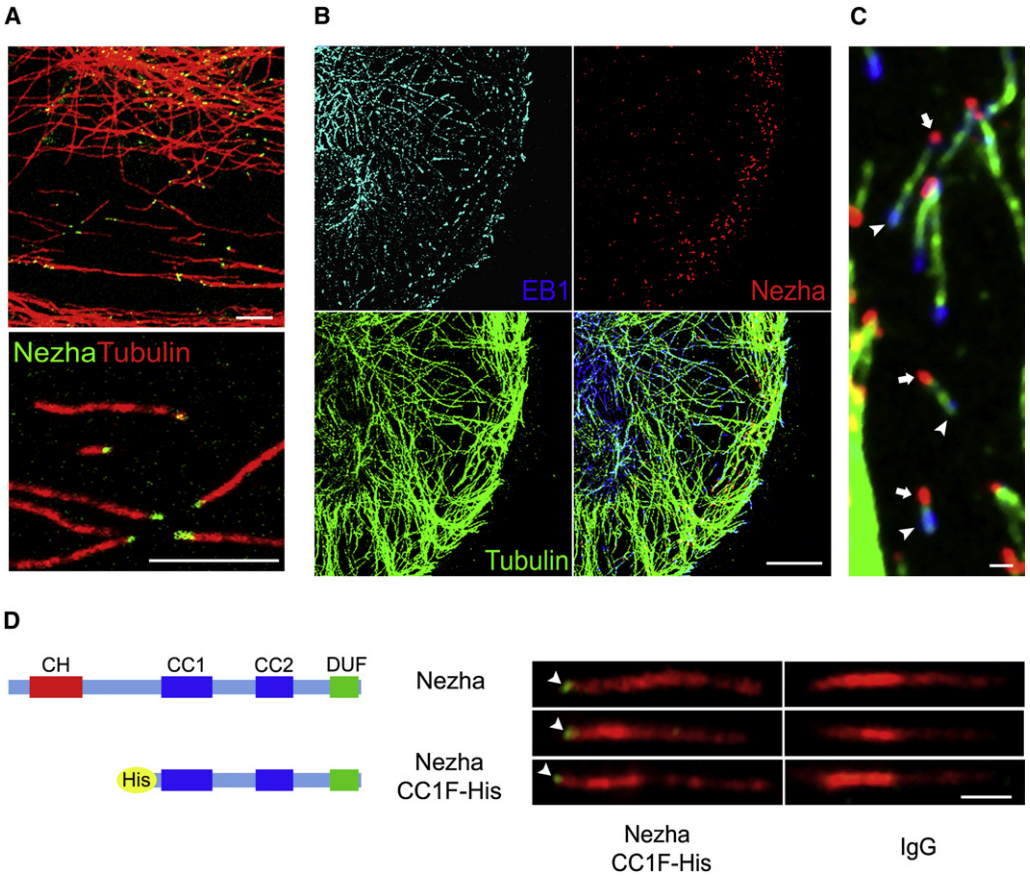

Figure 3. Nezha Localizes at Noncentrosomal MT Minus Ends

(A) Nezha localizes at one end of MTs. Caco2 cells were double-immunostained for Nezha and α-tubulin. The lower photo is an enlargement of part of the upper one.

(B) Nezha and EB1 are differentially localized. Caco2 cells were triple-immunostained for Nezha, α-tubulin, and EB1.

(C) Higher-magnification image of a cell stained as in (B). Each set of arrow and arrowhead points to Nezha and EB1 signals, respectively, localized on the opposite ends of a noncentrosomal MT.

(D) In vitro MT capping experiments. Structural views of Nezha and its His-tagged fragment used for this study are shown. MTs were sequentially polymerized with rhodamine-labeled tubulins and nonlabeled ones in the presence of Alexa 488-labeled His-Nezha-CC1F or mouse IgGs. Nezha-CC1F (green) marks the brighter seed ends, as indicated by the arrowheads. Approximately 35% of MTs were associated with Nezha, and out of them, 67% were attached to Nezha at the brighter end, with the others attached to unspecified positions.

Scale bars: 5 μm (A and B) and 1 μm (C and D).

Nezha (Figure S5A), and constructed an Alexa 488-labeled, His-tagged Nezha-CC1F recombinant protein (Figure 3D). To a solution of this protein, rhodamine-labeled and unlabeled tubulins were sequentially added. This protocol led to the production of chimeric MTs with high and low rhodamine intensities, in which the portion with brighter rhodamine signals corresponded to the minus-end side (Wiese and Zheng, 2000). We found that Nezha-CC1F was consistently localized at the brighter end of the chimeric MTs (Figure 3D). Thus, we could biochemically confirm that Nezha bound the MT minus end.

Dynamics of MTs Anchored at Nezha

To observe Nezha and associated MTs in living cells, we doubly transfected Caco2 cells with kusabira orange-labeled Nezha (Nezha-KOR) and GFP-α-tubulin and recorded their behavior by time-lapse movies, choosing thin peripheries of cells, which allowed us to obtain high-resolution imaging. These movies showed intriguing dynamics of these molecules: Individual Nezha puncta were located at an almost fixed position, and from each punctum, a single MT emerged, which showed repeated extension and retraction (Figure 4A and Movie S1). These results suggest that Nezha provided an anchoring point for the minus ends of MTs, allowing their dynamic elongation and shortening.

We also observed the dynamics of MT plus ends in relation to Nezha by doubly introducing EB1- or EB3-GFP and Nezha-KOR into Caco2 cells. The movie showed that a novel EB1 signal appeared directly from a Nezha-positive site and moved away, and this process was repeated (Figure 4B and Movie S2). These results confirmed that Nezha or Nezha-bearing structures sustained the repetitive plus-end growth of MTs. In this imaging, on the other hand, we did not distinguish whether the observed Nezha signals were derived from the ones localized in the cell

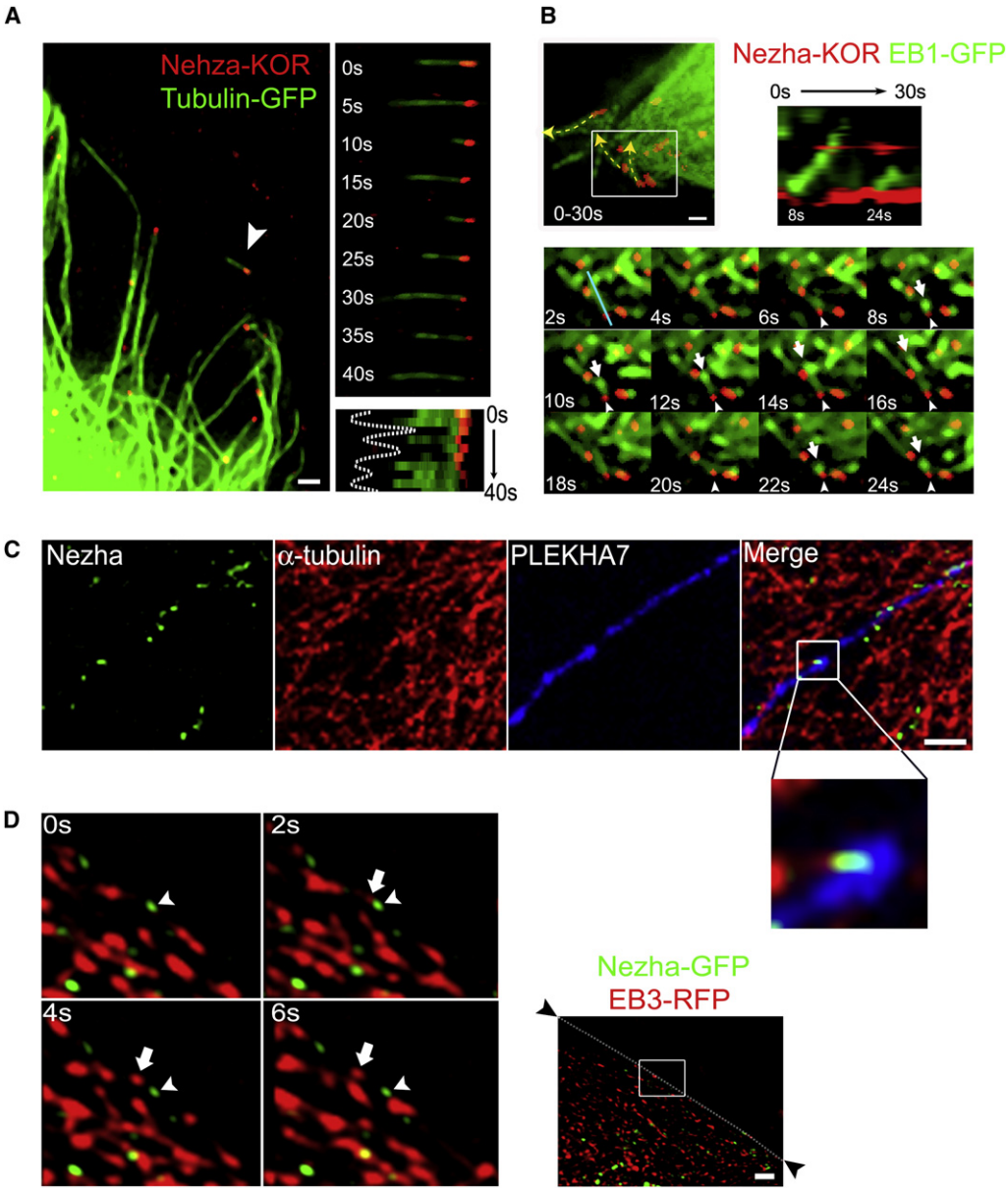

Figure 4. Dynamics of MTs Anchored at Nezha

(A) Time-lapse recording of Nezha-kusabira orange (KOR) and α-tubulin-GFP expressed in a Caco2 cell (see also Movie S1). Montage images (upper right) and kymograph (lower right) of the Nezha-MT complex indicated by the arrowhead are shown. Broken line shows the dynamics of the plus end.

(B) Time-lapse recording of Nezha-KOR and EB1-GFP expressed in a Caco2 cell. Upper left, reconstruction image of Movie S2. Yellow broken arrows indicate three independent tracks of growing EB1. Upper right and lower, the boxed region is shown by montage images, as well as by kymograph sampled at the cyan line. White arrows indicate the growing and regrowing MT plus ends, and arrowheads point to a Nezha-positive structure.

(C) Nezha-MT complexes localize on PLEKHA7 signals at cell junctions. Caco2 cells were triple-immunostained for Nezha, α-tubulin, and PLEKHA7. The boxed region was enlarged below.

(D) Time-lapse recording of a junctional Nezha-MT complex. Nezha-GFP and EB3-RFP were doubly expressed in a Caco2 cell, and images were acquired at 2 s intervals. Montage images of the region boxed in the right panel are shown. Arrowheads indicate a fixed Nezha signal, and arrows point to EB3 signals growing out of the Nezha signal. Dark arrowheads and the dotted line indicate the boundary of the transfected cell and nontransfected cell in contact with each other. Scale bars: 2 μm.

junctions or not. To analyze the interactions between Nezha and MTs at cell junctions, we triple-immunostained for Nezha, PLEKHA7, and MTs and found that the Nezha-MT complexes were localized in the PLEKHA7-positive zones (Figure 4C), supporting the model that these complexes were associated with PLEKHA7. We also purposely chose Nezha signals located at cell-cell boundaries for time-lapse recording and found a similar movement of EB1 or EB3 away from these Nezha puncta (Figure 4D).

KIFC3 Is Recruited to the Zonula Adherens in a PLEKHA7/Nezha-Dependent Manner

It was previously shown that dynein, a minus end-directed motor, was localized in cell junctions (Ligon et al., 2001). This led us to consider the possibility that a function of the MTs tethered to the PLEKHA7-Nezha complex at the minus end is to provide a track for dynein or other minus end-directed motors to reach the AJs. We therefore tested this possibility and actually found that KIFC3 (Yang et al., 1997), a minus end-directed motor, was localized along the ZA of Caco2 cells (Figure 5A), as well as in the centrosomes (Figure S8A). This junctional localization of KIFC3 was evident only at mature cell junctions, as in the case of Nezha. When PLEKHA7 or Nezha had been deleted, KIFC3 was diminished at cell junctions but not at the centrosomes (Figure 5B). In addition, overexpressed PLEKHA7 enhanced the recruitment of KIFC3 to the ZA in early cultures, where its accumulation to cell junctions was still incomplete; likewise, overexpression of Nezha, which induced MT bundling, recruited KIFC3 to the Nezha-positive sites (Figure S8B). All these observations suggest that KIFC3 was transported to cell junctions in a manner dependent on the PLEKHA7-Nezha complex.

Next, we attempted to visualize the KIFC3 recruitment to cell junctions by live-cell imaging: We doubly transfected Caco2 cells with EGFP-tagged KIFC3 (KIFC3-GFP) and kusabira orange-tagged E-cadherin (Ecad-KOR) and observed their behavior by time-lapse recording. The movies showed that, although exogenous KIFC3 tended to form static aggregates, there was a population of small KIFC3 clusters that actively moved from the cytoplasmic zones to the E-cadherin-positive junction and then settled there (Figure 5C and Movie S3). When the KIFC3 clusters below 0.27 μm in diameter were chosen for measurement, 36% of them showed such movement with a speed of 216 ± 81.9 nm/s (mean ± standard deviation [SD], n = 20). Such translocation of cytoplasmic KIFC3 to the cell junction was, however, not observed in nocodazole-treated transfectants (see below). We also observed that KIFC3 signals were associated with MTs oriented toward cell junctions in fixed samples (Figure 5D).

To examine the function of KIFC3, we knocked down its expression in Caco2 cells by using KIFC3-specific siRNA. After the KIFC3 depletion, E-cadherin signals at the ZA were disorganized (Figure 5E), as observed in PLEKHA7- or Nezha-depleted cells, suggesting that PLEKHA7, Nezha, and KIFC3 work together for the regulation of cadherin assembly at the ZA.

Microtubules Are Essential in the Actions of the Nezha-KIFC3 System

We examined how MTs themselves were involved in the above systems. We treated Caco2 cells with 10 to 20 μM nocodazole for 30 min to 6 hr and observed the junctional distributions of the proteins studied above. MT depolymerization began within 30 min, progressively affecting the distribution of Nezha, KIFC3, and PLEKHA7/E-cadherin in this sequence: Nezha signals disappeared from cell-cell boundaries by 30 min (Figure S9A), indicating that the junctional localization of Nezha depended on its binding to MTs. KIFC3 signals began to be disorganized at 1 hr and disappeared by 2 hr from the junctions (Figure S9B); concomitantly, their movement toward the junction ceased, as mentioned above. During these incubation times, the localization of PLEKHA7 and E-cadherin appeared to be unchanged. At 6 hr, however, PLEKHA7 signals became zigzag or fragmented, and E-cadherin delineating the ZA became reduced and discontinuous (Figures S9C and S9D). These results confirmed the specific requirement of MTs for the ZA assembly but simultaneously indicated that the sensitivity of these proteins to MT depolymerization differed. The delayed response of E-cadherin could be explained by its half-life in epithelial junctions, which was estimated to be about 6 hr (Troxell et al., 1999); that is, only the E-cadherin molecules newly redistributing to the junctions might have been affected by the nocodazole treatment.

The above studies suggest that KIFC3 utilized the Nezha-anchored MTs for accessing the junctions. If this is the case, KIFC3 would be expected to behave differently from other junctional proteins during their relocation to the junctions. We tested this possibility by FRAP (fluorescence recovery after photobleaching). The results revealed that the behavior of KIFC3 was unique, displaying a higher repopulation rate compared with those of p120, PLEKHA7, and E-cadherin (Figure S10). Furthermore, during the image capturing, we frequently observed that KIFC3 puncta moved directly into the photobleached zones of the junction from the cytoplasm. These observations support the hypothesis that KIFC3 was distributed to the junction via a specific route, likely MTs.

Finally, we compared the morphology of Caco2 cells after depletion of these proteins by immunostaining for ZO-1, which delineates the apical outline of epithelial cells. In all these cells, the apical surface area was significantly expanded (Figure S11) with concomitant flattening of the cells, suggesting that the PLEKHA7-Nezha-KIFC3-dependent system is critical for cells to maintain proper tension.

DISCUSSION

The mechanisms governing which subcellular structures or molecules regulate the dynamics of noncentrosomal MTs in epithelial cells have not been well understood. In the present study, we identified a novel protein, Nezha, that can anchor the MT minus ends to noncentrosomal structures and therefore explored its biological functions.

Nezha as a Regulator of MT Dynamics

The present studies have provided evidence that Nezha binds noncentrosomal MTs via their minus ends. It is thought that noncentrosomal MTs are generated by release from the centrosomes or become nucleated from some noncentrosomal sites (Bartolini and Gundersen, 2006; Mogensen and Tucker, 1987; Vorobjev et al., 1997; Yvon and Wadsworth, 1997). In our live imaging of cells cotransfected with EB1 and Nezha, EB1 signals appeared to emerge de novo from the sites where Nezha was localized. These images suggest that Nezha may function as an MT-nucleation center, rather than for simple anchoring of pre-existing MTs. Whether Nezha has indeed a nucleation activity, however, remains to be further investigated. It is also undetermined whether Nezha organizes a subcellular structure together with other proteins. Ninein is known to capture MTs at their minus ends, like Nezha, suggesting their possible cooperation. In our immunostaining experiments, however, Nezha did

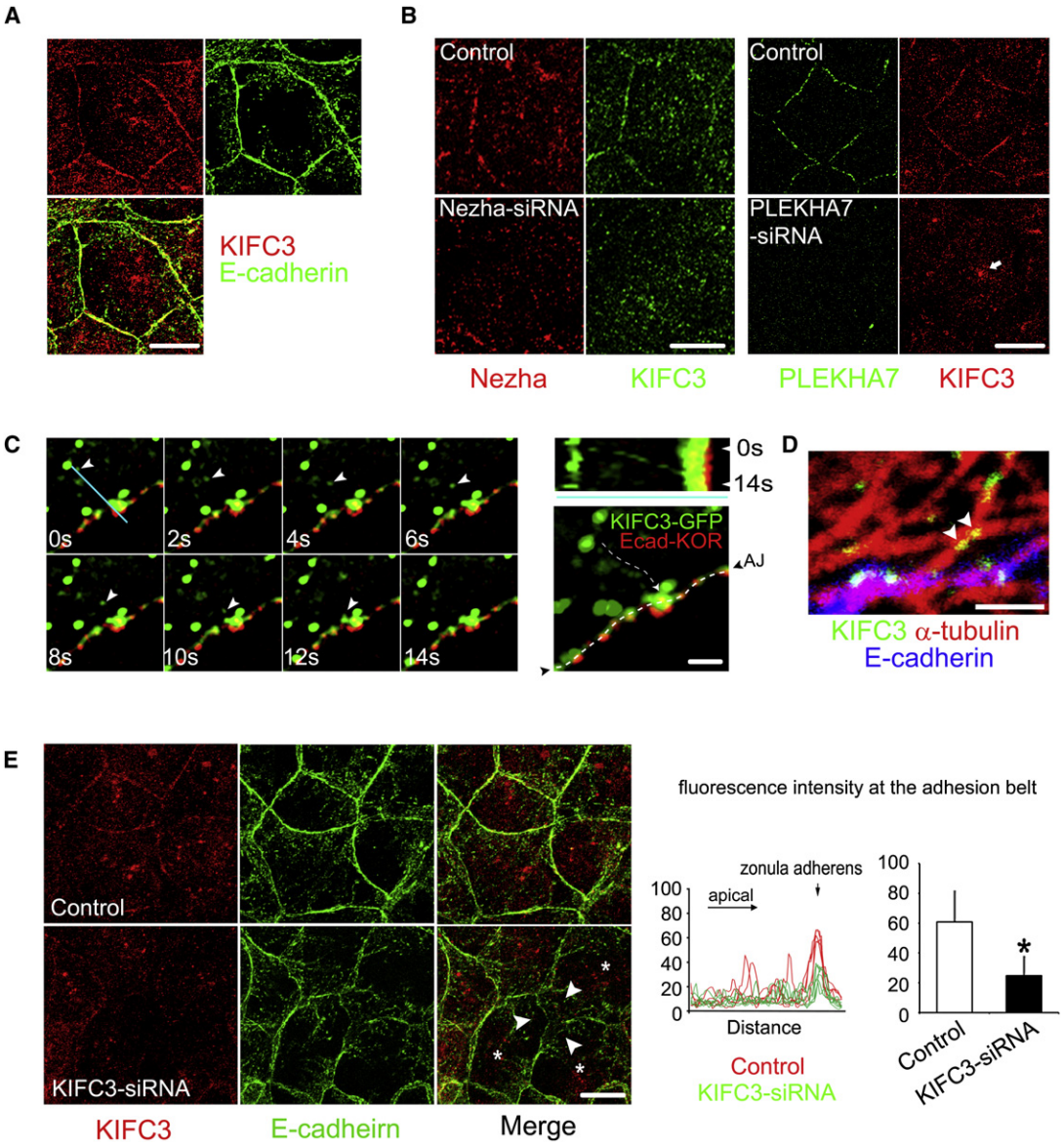

Figure 5. KIFC3 Is Recruited to the Zonula Adherens

(A) KIFC3 localizes along the ZA. Caco2 cells were doubly immunostained for KIFC3 and E-cadherin.

(B) The junctional distribution of KIFC3 depends on PLEKHA7 and Nezha. Caco2 cells were transfected with control, PLEKHA7, or Nezha siRNA. KIFC3 became undetectable at cell junctions after PLEKHA7 or Nezha depletion but was still detectable at the centrosomes (arrow).

(C) Time-lapse recording of KIFC3-GFP and E-cadherin-KOR expressed in a Caco2 cell. Left, montage images of Movie S3. Arrowheads indicate KIFC3-GFP signals moving toward the E-cadherin-positive junction. Upper right, kymograph for the KIFC3-GFP signals sampled at the cyan line indicated in the 0 s montage image. Lower right, reconstruction image of the movie, in which the broken arrow indicates the track of moving KIFC3 signals. Broken lines indicate the ZA.

(D) Triple-immunostaining for endogenous KIFC3, MTs, and E-cadherin. Arrowheads indicate KIFC3 signals localized on a MT, which is associated with an E-cadherin-positive site.

(E) KIFC3 depletion disorganizes E-cadherin assembly. Caco2 cells were transfected with control or KIFC3 siRNA. As indicated by the arrowheads, E-cadherin signals were disorganized in the junctions formed between KIFC3-knocked down cells (marked with asterisks). The amount of E-cadherin at the ZA was quantified. *$p < 0.01$, $n = 3$ independent experiments (50 cells/n). Error bars represent the SD.

Scale bars: 10 μm (A, B, and E) and 1 μm (C and D).

not colocalize with ninein, suggesting that Nezha plays a unique role, distinct from that of ninein.

We found two pools of Nezha, junctional and cytoplasmic. The junctional Nezha was recruited to this site via its interaction with PLEKHA7. With regard to the cytoplasmic Nezha, we did not identify the mechanism as to how it was localized in the cytoplasm. Although Nezha may have a similar function in the junctional and nonjunctional sites, the present study was focused on the junction-located Nezha.

Nezha as a Component of the Adherens Junction

We first identified PLEKHA7 as a protein that interacted with p120 and then Nezha as a PLEKHA7-binding partner. Since PLEKHA7 was coimmunoprecipitated not only with p120 and Nezha but also with E-cadherin, we can imagine the presence of a molecular complex linked in the sequence of E-cadherin-p120-PLEKHA7-Nezha, although the possibility that the PLEKHA7-Nezha complex was present in the junctions independently of the E-cadhein-p120-PLEKHA7 complex could not be excluded. The association of Nezha with the junctions was MT dependent. This finding suggests that a cooperative interaction between Nezha and MTs regulates the binding of Nezha to PLEKHA7. Both PLEKHA7 and MTs bound the C-terminal region of Nezha, suggesting that their interactions with Nezha occur at a nearby location; and this observation can be taken as a clue for our future analysis of the cooperativity. Another important observation was that PLEKHA7 and Nezha were strictly localized along the ZA, despite the fact that p120 was distributed throughout cell-cell contacts, as were E-cadherin and other catenins. There must be a mechanism to confer a specific property on the cadherin-catenin complex to allow it to associate with these proteins only at the ZA. In addition, it should be noted that p120 (Chartier et al., 2007; Franz and Ridley, 2004; Ichii and Takeichi, 2007) and PLEKHA7, as well as KIFC3, were capable of localizing in the centrosomes, suggesting a potential role of these proteins in the centrosomes.

The role of p120 in cadherin-based junction formation has been extensively studied, and one of its major functions is to stabilize cadherin turnover in the cell membrane (Reynolds, 2007). Whereas this role of p120 depends on the centrally located armadillo domain (Liu et al., 2007), the site required for the interaction of p120 with PLEKHA7 resides in the N-terminal domain. Thus, our present study has identified a novel p120-dependent mechanism for regulation of cell-cell contacts.

Nezha Cooperates with KIFC3 for the Maintenance of the Zonula Adherens

Consistent with the localization of PLEKHA7 and Nezha, their depletion selectively affected the E-cadherin-catenin complex localized at the ZA, but not its entire populations present at the cell-cell contacts, highlighting that the PLEKHA7-Nezha system is solely important for the integrity of the ZA. Then, how are the Nezha-anchored MTs involved in this process? We found that KIFC3 was localized along the ZA and demonstrated that KIFC3 was moving to the junctions from the cytoplasm. This movement was most likely MT dependent because it was blocked with nocodazole, although it remained unclear whether KIFC3 "migrated" on MTs in the same way as other kinesin motors do or interacted with MTs in some distinct manner. FRAP analysis also indicated that KIFC3 was redistributed to the junctions via a unique route. Importantly, KIFC3 depletion affected cell junctions as did Nezha or PLEKHA7 depletion. This fact suggests that KIFC3 is part of the PLEKHA7-Nezha-MT machinery. Supporting this idea, MT depolymerization itself affected the junction integrity in a pattern similar to that observed after the depletion of PLEKHA7, Nezha, and KIFC3.

The detailed role of KIFC3, on the other hand, remains to be explored. According to a previous report (Noda et al., 2001), KIFC3 is associated with apically transported vesicles. Such vesicles may contain molecules necessary for the maintenance of the ZA. We have never observed E-cadherin signals moving together with KIFC3 in the cytoplasm, and therefore something else might be transported by this motor protein. It is noteworthy that the cell surface population of E-cadherin was not reduced by depletion of PLEKHA7, Nezha, or KIFC3 (W.M., unpublished data), suggesting that the system disclosed here is likely not important for the trafficking of cadherin molecules. On the other hand, we cannot exclude the possibility that KIFC3 functions as a regulatory or structural element of the adhesion protein complex rather than as a cargo motor.

The Roles of Microtubules in the Cadherin-Based Junctions

The involvement of MTs in AJ organization has already been reported. For example, nocodazole treatment perturbs the ability of cells to accumulate E-cadherin at cell-cell contacts in mammary tumor cell lines (Stehbens et al., 2006), results that are at least in part consistent with ours. However, in such studies, the potential interactions of MT plus ends with cell junctions were the matter of focus, and importantly, p120 was found not to be required for these interactions. Thus, these and our results suggest that p120 contributes to only the minus end-dependent interactions of MTs with AJs. It is possible that both the MT minus and plus ends play roles in AJ assembly, but likely in different ways. Another report demonstrated that MT minus ends are stabilized by the presence of cadherin-mediated junctions (Chausovsky et al., 2000). This phenomenon might be explained by assuming that the junction-associated Nezha plays a role in the stabilization of the minus ends.

It should be stressed that Nezha and KIFC3 were recruited to cell junctions only in the mature cell-cell contacts. The MT-dependent system disclosed in this study is therefore likely important for the maintenance or modulation of mature AJs rather than for the initiation of their formation. When these proteins were removed, the apical area of Caco2 cells was expanded, suggesting that the cells lost tension to maintain their morphology. It is intriguing to study how such cell biological effects affect tissue morphogenesis in vivo. Our preliminary observations of the tissue distribution of Nezha in mouse embryos indicate that this protein is expressed by various cell types including neuronal cells, implying that it may have diverse functions. It should also be re-emphasized that Nezha was distributed not only in the junctions but also in other sites in the cells, and therefore this protein likely plays a role at those sites, too, for MT minus-end regulation. Further analysis of Nezha and associated proteins may contribute to our deeper understanding of the dynamics and roles of MT minus ends that are not anchored to the centrosomes.

EXPERIMENTAL PROCEDURES

Plasmids

cDNA clones of human PLEKHA7 and mouse Nezha were obtained from the Mammalian Gene Collection. For preparation of tagged constructs, PLEKHA7 was cloned into pEGFP (Clontech) or pCMVtag 2B (Stratagene) by PCR with a DNA fragment set of 5′-ATAAAGCTTAACATGGCGGCGGCGACGGTC-3′ and 3′-ATACTCGAGACATACTGAGCCAAGATCTCC-5′; and Nezha was

cloned into pEGFP or pmKO1-MC1(MBL) by PCR with that of ATAAGATC TATGGTGGAAGCGGCGCCC'-3′ and 3′-ATAGTCGACTTTGGGGGTACCGC CACC-5′. Their fragments were subcloned into the pEGFP vector with a GFP-tag sequence on its 5′ end or into the PQE30 vector (QIAGEN) with a His tag sequence on its 3′ end. A cDNA clone of human KIFC3 was kindly provided by N. Hirokawa (University of Tokyo), and it was subcloned into pEGFPC1. N-cadherin and its mutant, cN/JM(-) (Aono et al., 1999), were subcloned into the pCA vector. Mouse p120 N-terminal (aa 1–346) and C-terminal (aa 347–921) fragments were subcloned into PGEX-6P-1(GE Healthcare). EB1-GFP and EB3-RFP were kindly given to us by Y. Mimori-Kiyosue (KAN Institute). Human α-tubulin-pCAsalGFP and mouse E-cadherin pmKO1-MC1, constructed by Y. Kametani, were used for imaging assays. The following siRNAs were used: siPLEKHA7-1, 5′-CCACGCUGUCAAGAACUCAUCUCAU-3′; siPLEKHA7-2, 5′-GAGAGCGACACUGACGUCAAACUGA-3′; siNezha-1, 5′-CAGCAGCCACCAACUCCGAGGUGAA-3′; siNezha-2, 5′-CAGAACGCAAGA AACAGCUGGUGAA-3′; sip120-1, 5′-GGCUAGAGGAUGACCAGCGUAGUAU -3′; and sip120-2, 5′- GCAGCUCCCAAUGUUGCCAACAAUA-3′ (Stealth siRNAs, Invitrogen); siKIFC3-1, 5′-GUUUGAGUUUGGCCACACUUU-3′; and siKIFC3-2, 5′- GAAACAUGUUCAGAAGGAAUU-3′ (MISSION siRNAs, SIGMA). Negative-control stealth siRNAs were also obtained for the respective siRNAs from Invitrogen or SIGMA.

Antibodies

Mouse monoclonal antibodies (mAbs) against a C-terminal portion (aa 721–1121) of human PLEKHA7 or an N-terminal portion (aa 18–206) of mouse Nezha were generated. Rabbit or rat polyclonal antibodies (pAbs) against a C-terminal sequence (CPASYGPGEQNGTGGY) of human PLEKHA7 and a C-terminal sequence (SRLPGSRERDWENG) of mouse Nezha were also generated and affinity-purified with antigen-coupled CH-Sepharose beads (GE Healthcare), as described previously (Otani et al., 2006). The following antibodies were also used: mouse mAb HECD-1 against human E-cadherin (Shimoyama et al., 1989); rat mAb ECCD2 against mouse E-cadherin (Shirayoshi et al., 1986); mouse mAbs against p120-catenin and EB1 (BD Biosciences); mouse mAb (Roche) and rabbit pAb (Chemicon) against GFP; mouse mAb and rabbit pAb against ZO-1 (Zymed); mouse mAb (DM1A, Sigma-Aldrich), rat mAb (YL1/2, Chemicon), and rabbit pAb (Cell Signaling) against α-tubulin; mouse mAb against desmoplakin 1 and 2 (Progene); and rabbit pAb against ninein (BIOLEGEND). The following secondary antibodies were used: goat Alexa Fluor 488/594-conjugated anti-mouse or anti-rabbit IgG (Invitrogen); sheep HRP-conjugated anti-mouse or anti-rabbit IgG (GE Healthcare); Alexa Fluor 488-, 555-, 594-, or 647-conjugated secondary antibody (Molecular Probes); Cy3-conjugated anti-rat IgG (Chemicon); peroxidase-conjugated anti-rat IgG (Jackson); and peroxidase-conjugated anti-mouse or anti-rabbit IgG (GE Healthcare).

Cell Culture and Transfection

Cells were cultured at an initial density of $5 \times 10^4/cm^2$ in collagen-coated dishes, with a 1:1 mixture of DME and Ham's F12 supplemented with 10% FCS. Cells at approximately 70% confluence were transfected by use of FuGENE HD (Roche). For isolating stable transfectants, cells were exposed to 400 μg/ml G418. For siRNA treatments, cells were transfected by using Lipofectamine 2000 (Invitrogen). We generally obtained more than 90% reduction in the protein level for the siRNAs used at 4 to 6 days after transfection, unless otherwise noted, and we examined the effects of RNA interference at 5 days.

Immunofluorescence Staining

Cells were fixed and immunostained as described earlier (Otani et al., 2006). Preparations were analyzed by using a laser-scanning confocal microscope (LSM 510 mounted on an Axiovert 100M microscope, Carl Zeiss MicroImaging) on an inverted stand with C-Apochromat 40×/1.20 and Plan-Apochromat 63×/1.40 objectives (Carl Zeiss MicroImaging).

Biochemical Assays

For immunoprecipitation, cells were lysed in a lysis buffer (50 mM Tris-HCl, pH 7.5, containing 50 mM NaCl, 0.5 mM EDTA, 0.5 mM EGTA, 1.5 mM $MgCl_2$, 1 mM DTT, and 0.5% Triton X-100). Lysates, precleared with protein G-Sepharose 4FF beads (GE Healthcare), were incubated with anti-Flag mAb antibody or anti-Nezha pAb for 1 hr, followed by incubation with protein G-Sepharose beads for 1 hr. The beads were subsequently washed three times in the lysis buffer. For pulldown assays, cells were lysed in the HS-buffer (20 mM Tris-HCl, pH 7.4, containing 500 mM NaCl, 5 mM $MgCl_2$, and 1% Triton X-100). GST proteins (10 μg) were added to the lysate. After a 1 hr incubation, the lysate was incubated for another 1 hr with glutathione-Sepharose 4B beads (GE Healthcare). The beads were subsequently washed in HS buffer.

Preparation of Recombinant Nezha-CC1F-His and Capping Experiments

Fusion proteins were purified by using a His-Trap column (GE Healthcare) and subjected to labeling with Alexa Fluor-488 Protein Labeling kit (Invitrogen). The in vitro microtubule-capping experiment was performed as described previously (Wiese and Zheng, 2000). Briefly, we mixed 4 μl of 2 mg/ml rhodamine-labeled tubulin (Cytoskeleton) and 1 μl of 2 nM Alexa 488-labeled Nezha-CC1F-His, both of which contained 10 μM Taxol. This mixture was incubated for 5 min at 37°C, and then 3 volumes of nonlabeled tubulin, prepared from rat brains as described earlier (Maekawa et al., 2001), were added. After another 15 min incubation at 37°C, the reaction was stopped by adding 10 volumes of 1% glutaraldehyde at 23°C and incubating the mixture for 3 min, and then the solution was diluted with 250 μl of 80% glycerol in BRB80. Each reaction mixture was spotted onto a microscope slide, covered with a coverslip, and viewed under an epifluorescence microscope through a Plan Apochromat 63×/1.4 lens (Carl Zeiss).

Live-Cell Imaging, Image Processing, and Statistical Analysis

Live-cell imaging was performed by using a Delta Vision microscope (Applied Precision), and the digital images thus obtained were analyzed as described previously (Kametani and Takeichi, 2007). Time-lapse image series were acquired at 2 s or 5 s intervals at 37°C. Fluorescence intensity and cell-surface areas were measured by using Image J. All statistical analysis was performed by using Student's t test with Excel (Microsoft). Error bars in the figures represent ± SD.

SUPPLEMENTAL DATA

Supplemental Data include Supplemental Experimental Procedures, 11 figures, and three movies and can be found with this article online at http://www.cell.com/supplemental/S0092-8674(08)01197-5.

ACKNOWLEDGMENTS

We thank Y. Mimori-Kiyosue for advice, N. Hirokawa for KIFC3 antibody and cDNA, and K. Shinmyozu for mass spectrometric analysis. We are also grateful to C. Yoshii, H. Abe-Ishigami, and M. Nomura-Harata for their technical support, as well as other members of our laboratory for discussion. This work was supported by a grant from the program Grants-in-Aid for Specially Promoted Research of the Ministry of Education, Science, Sports, and Culture of Japan.

Received: May 13, 2008
Revised: August 20, 2008
Accepted: September 17, 2008
Published: November 26, 2008

REFERENCES

Akhmanova, A., and Hoogenraad, C.C. (2005). Microtubule plus-end-tracking proteins: mechanisms and functions. Curr. Opin. Cell Biol. *17*, 47–54.

Aono, S., Nakagawa, S., Reynolds, A.B., and Takeichi, M. (1999). p120(ctn) acts as an inhibitory regulator of cadherin function in colon carcinoma cells. J. Cell Biol. *145*, 551–562.

Bacallao, R., Antony, C., Dotti, C., Karsenti, E., Stelzer, E.H., and Simons, K. (1989). The subcellular organization of Madin-Darby canine kidney cells during the formation of a polarized epithelium. J. Cell Biol. *109*, 2817–2832.

Bartolini, F., and Gundersen, G.G. (2006). Generation of noncentrosomal microtubule arrays. J. Cell Sci. *119*, 4155–4163.

Chartier, N.T., Oddou, C.I., Laine, M.G., Ducarouge, B., Marie, C.A., Block, M.R., and Jacquier-Sarlin, M.R. (2007). Cyclin-dependent kinase 2/cyclin E complex is involved in p120 catenin (p120ctn)-dependent cell growth control: a new role for p120ctn in cancer. Cancer Res. *67*, 9781–9790.

Chausovsky, A., Bershadsky, A.D., and Borisy, G.G. (2000). Cadherin-mediated regulation of microtubule dynamics. Nat. Cell Biol. *2*, 797–804.

Chen, X., Kojima, S., Borisy, G.G., and Green, K.J. (2003). p120 catenin associates with kinesin and facilitates the transport of cadherin-catenin complexes to intercellular junctions. J. Cell Biol. *163*, 547–557.

Dammermann, A., Desai, A., and Oegema, K. (2003). The minus end in sight. Curr. Biol. *13*, R614–R624.

Franz, C.M., and Ridley, A.J. (2004). p120 catenin associates with microtubules: inverse relationship between microtubule binding and Rho GTPase regulation. J. Biol. Chem. *279*, 6588–6594.

Gerhard, D.S., Wagner, L., Feingold, E.A., Shenmen, C.M., Grouse, L.H., Schuler, G., Klein, S.L., Old, S., Rasooly, R., Good, P., et al. (2004). The status, quality, and expansion of the NIH full-length cDNA project: the Mammalian Gene Collection (MGC). Genome Res. *14*, 2121–2127.

Ichii, T., and Takeichi, M. (2007). p120-catenin regulates microtubule dynamics and cell migration in a cadherin-independent manner. Genes Cells *12*, 827–839.

Kametani, Y., and Takeichi, M. (2007). Basal-to-apical cadherin flow at cell junctions. Nat. Cell Biol. *9*, 92–98.

Kaufmann, U., Kirsch, J., Irintchev, A., Wernig, A., and Starzinski-Powitz, A. (1999). The M-cadherin catenin complex interacts with microtubules in skeletal muscle cells: implications for the fusion of myoblasts. J. Cell Sci. *112*, 55–68.

Lechler, T., and Fuchs, E. (2007). Desmoplakin: an unexpected regulator of microtubule organization in the epidermis. J. Cell Biol. *176*, 147–154.

Ligon, L.A., Karki, S., Tokito, M., and Holzbaur, E.L. (2001). Dynein binds to beta-catenin and may tether microtubules at adherens junctions. Nat. Cell Biol. *3*, 913–917.

Liu, H., Komiya, S., Shimizu, M., Fukunaga, Y., and Nagafuchi, A. (2007). Involvement of p120 carboxy-terminal domain in cadherin trafficking. Cell Struct. Funct. *32*, 127–137.

Maekawa, S., Morii, H., Kumanogoh, H., Sano, M., Naruse, Y., Sokawa, Y., and Mori, N. (2001). Localization of neuronal growth-associated, microtubule-destabilizing factor SCG10 in brain-derived raft membrane microdomains. J. Biochem. (Tokyo) *129*, 691–697.

Mary, S., Charrasse, S., Meriane, M., Comunale, F., Travo, P., Blangy, A., and Gauthier-Rouviere, C. (2002). Biogenesis of N-cadherin-dependent cell-cell contacts in living fibroblasts is a microtubule-dependent kinesin-driven mechanism. Mol. Biol. Cell *13*, 285–301.

Mimori-Kiyosue, Y., Shiina, N., and Tsukita, S. (2000). The dynamic behavior of the APC-binding protein EB1 on the distal ends of microtubules. Curr. Biol. *10*, 865–868.

Mogensen, M.M., and Tucker, J.B. (1987). Evidence for microtubule nucleation at plasma membrane-associated sites in Drosophila. J. Cell Sci. *88*, 95–107.

Mogensen, M.M., Malik, A., Piel, M., Bouckson-Castaing, V., and Bornens, M. (2000). Microtubule minus-end anchorage at centrosomal and non-centrosomal sites: the role of ninein. J. Cell Sci. *113*, 3013–3023.

Noda, Y., Okada, Y., Saito, N., Setou, M., Xu, Y., Zhang, Z., and Hirokawa, N. (2001). KIFC3, a microtubule minus end-directed motor for the apical transport of annexin XIIIb-associated Triton-insoluble membranes. J. Cell Biol. *155*, 77–88.

Otani, T., Ichii, T., Aono, S., and Takeichi, M. (2006). Cdc42 GEF Tuba regulates the junctional configuration of simple epithelial cells. J. Cell Biol. *175*, 135–146.

Reynolds, A.B. (2007). p120-catenin: Past and present. Biochim. Biophys. Acta *1773*, 2–7.

Shaw, R.M., Fay, A.J., Puthenveedu, M.A., von Zastrow, M., Jan, Y.N., and Jan, L.Y. (2007). Microtubule plus-end-tracking proteins target gap junctions directly from the cell interior to adherens junctions. Cell *128*, 547–560.

Shimoyama, Y., Hirohashi, S., Hirano, S., Noguchi, M., Shimosato, Y., Takeichi, M., and Abe, O. (1989). Cadherin cell-adhesion molecules in human epithelial tissues and carcinomas. Cancer Res. *49*, 2128–2133.

Shirayoshi, Y., Nose, A., Iwasaki, K., and Takeichi, M. (1986). N-linked oligosaccharides are not involved in the function of a cell-cell binding glycoprotein E-cadherin. Cell Struct. Funct. *11*, 245–252.

Stehbens, S.J., Paterson, A.D., Crampton, M.S., Shewan, A.M., Ferguson, C., Akhmanova, A., Parton, R.G., and Yap, A.S. (2006). Dynamic microtubules regulate the local concentration of E-cadherin at cell-cell contacts. J. Cell Sci. *119*, 1801–1811.

Strausberg, R.L., Feingold, E.A., Grouse, L.H., Derge, J.G., Klausner, R.D., Collins, F.S., Wagner, L., Shenmen, C.M., Schuler, G.D., Altschul, S.F., et al. (2002). Generation and initial analysis of more than 15,000 full-length human and mouse cDNA sequences. Proc. Natl. Acad. Sci. USA *99*, 16899–16903.

Su, L.K., Burrell, M., Hill, D.E., Gyuris, J., Brent, R., Wiltshire, R., Trent, J., Vogelstein, B., and Kinzler, K.W. (1995). APC binds to the novel protein EB1. Cancer Res. *55*, 2972–2977.

Teng, J., Rai, T., Tanaka, Y., Takei, Y., Nakata, T., Hirasawa, M., Kulkarni, A.B., and Hirokawa, N. (2005). The KIF3 motor transports N-cadherin and organizes the developing neuroepithelium. Nat. Cell Biol. *7*, 474–482.

Troxell, M.L., Chen, Y.T., Cobb, N., Nelson, W.J., and Marrs, J.A. (1999). Cadherin function in junctional complex rearrangement and posttranslational control of cadherin expression. Am. J. Physiol. *276*, C404–C418.

Vallee, R.B. (1982). A taxol-dependent procedure for the isolation of microtubules and microtubule-associated proteins (MAPs). J. Cell Biol. *92*, 435–442.

Vogelmann, R., and Nelson, W.J. (2005). Fractionation of the epithelial apical junctional complex: reassessment of protein distributions in different substructures. Mol. Biol. Cell *16*, 701–716.

Vorobjev, I.A., Svitkina, T.M., and Borisy, G.G. (1997). Cytoplasmic assembly of microtubules in cultured cells. J. Cell Sci. *110*, 2635–2645.

Waterman-Storer, C.M., Salmon, W.C., and Salmon, E.D. (2000). Feedback interactions between cell-cell adherens junctions and cytoskeletal dynamics in newt lung epithelial cells. Mol. Biol. Cell *11*, 2471–2483.

Wiese, C., and Zheng, Y. (2000). A new function for the gamma-tubulin ring complex as a microtubule minus-end cap. Nat. Cell Biol. *2*, 358–364.

Yanagisawa, M., Kaverina, I.N., Wang, A., Fujita, Y., Reynolds, A.B., and Anastasiadis, P.Z. (2004). A novel interaction between kinesin and p120 modulates p120 localization and function. J. Biol. Chem. *279*, 9512–9521.

Yang, Z., Hanlon, D.W., Marszalek, J.R., and Goldstein, L.S. (1997). Identification, partial characterization, and genetic mapping of kinesin-like protein genes in mouse. Genomics *45*, 123–131.

Yvon, A.M., and Wadsworth, P. (1997). Non-centrosomal microtubule formation and measurement of minus end microtubule dynamics in A498 cells. J. Cell Sci. *110*, 2391–2401.